REVISTA MATÉRIA V.22 N.04
ISSN 1517-7076 artigo e-11887, 2017

Theoretical study of c-GaN/GaAs single heterojunction solar cells

Ana Gabriela Galicia Cruz [1], Mario Díaz Solís [1], Leandro García González [1], Julián Hernández Torres [1], Máximo López López [2], Gerardo Contreras Puente [3], Guillermo Santana Rodríguez [4], Luis Zamora Peredo [1]

[1] Centro de Investigación en Micro y Nanotecnología, Universidad Veracruzana, CP: 94294, Boca del Río, VER
e-mail: gabgaliciac@gmail.com
[2] Physics Department, Centro de Investigación y de Estudios Avanzados del IPN, CP: 07360, México City
[3] Escuela Superior de Física y Matemáticas del IPN, CP: 07738, México City
[4] Instituto de Investigaciones em Materiales, Universidad Nacional Autónoma de México, CP: 04510, México City

ABSTRACT

In this work a theoretical study of electrical behavior for a c-GaN/GaAs heterostructure as a photovoltaic device through a two-dimensional (2D) finite element numerical simulation is presented for a first time. I-V curves and electrical parameters like short circuit current (Isc), open circuit voltage (Voc), fill factor (FF) and efficiency (η) were obtained for n-i-p and n-p heterostructures with different thicknesses and doping of the layers by modeling heterostructures with characteristics parameters of this materials previously reported. As a result, an increment on Isc was observed by extending the thickness of i-GaAs layer from 12 mA/cm^2 for thinner heterostructures to a maximum of ~32 mA/cm^2 for heterostructures with i-GaAs layer >3000 nm and a decrease in Voc and FF in the range from ~1.06 V and 0.89 for n-p heterostructures to 0.75 V and 0.7 respectively for thicker i-GaAs layers allowing estimate maximum efficiencies between 23 and 25% for n-i-p and n-p configurations, respectively. This study allows demonstrating the potential of this type of heterostructures for solar cells applications, considering the possibility of using p-doping GaAs substrates for photovoltaics based in GaN.

Keywords: GaN/GaAs, heterostructures, TCAD modeling, I-V curves, solar cell.

1. INTRODUCTION

At the last years, gallium nitride (GaN) has been considered a valuable material for development of photonic devices, due to its wide direct bandgap (3.2-3.4 eV), high absorption coefficient (105 cm-1 at the band edge) and radiation damage resistance [1,2]. On photovoltaic matters, GaN has been suitable to get InGaN alloys and to design III-nitride multi-junction solar cell structures for greatest efficiency [3]. However, the experimental results have showed low conversion efficiency due to some challenges in fabrication of GaN films (such as p-type doping control [4] and the lack of a suitable substrate [5]) and InGaN films (degradation of epitaxial quality at high In compositions [6]). At this point, gallium arsenide (GaAs) is an option that offers the possibility to evade both problems: p-GaN film and substrate. Nevertheless, there are some challenges in development of this heterostructures due to strain and defects originated on the interface by a large lattice constant mismatch between GaN and GaAs (~20% for cubic GaN [5]) and the mix of cubic and hexagonal phases in GaN [7]. Although several studies have reported structural characterization of GaN/GaAs heterojunctions with cubic (c-GaN) or hexagonal GaN (h-GaN) layers growth over GaAs substrates [8-9], with photovoltaic purposes there is not reports.

Based on this, the present work proposes a theoretical study by a two-dimensional (2D) finite element numerical simulation of a n-i-p GaN/GaAs heterostructure using cubic GaN (c-GaN) to estimate its electrical behavior, efficiency potential and feasibility of such a heterojunction for application in photovoltaic devices. In order to obtain a realistic prediction of photoelectrical behavior on simulated devices, wavelength dependent refractive index and absorption coefficient for GaN and GaAs are modeled; beside this, a set of characteristic parameters and physical models for recombination, mobility, and bandgap narrowing are implemented in this study. The importance of this research lies in being the first photovoltaic cell proposal that addresses the use of these materials in a single heterojunction.

Corresponding Author : Ana Gabriela Galicia Cruz Received on: 31/08/2016 Accepted on: 10/05/2017

10.1590/S1517-707620170004.0221

2. MATERIALS AND METHODS

Photovoltaic cells based on n-GaN/i-GaAs/p-GaAs heterostructures were modeled under different configurations by Silvaco Atlas TCAD Software. First, we explore the thickness effect of the layers whereas the doping was fixed at $1x10^{18}$, $1x10^{12}$ and $1x10^{19}$ atoms/cm^{-3} for n-, i-, and p-type layers, respectively, as shown in Figure 1a. And next, we fixed the doping of *i-GaAs* and *p-GaAs* layers and the thickness of the *n-GaN* layer at 300 nm; we changed the doping level in *n-GaN* layer for different thicknesses on *i-GaAs* and *p-GaAs* layers as shown in Figure 1b.

Modeling parameters for GaN and GaAs layers used in this simulations are summarized in Table 1. Wavelengh-dependent refractive index (n) and absorption coefficient (α) of GaN, were calculated with III-V compounds Adachi's model [10] and the equation proposed by Brown et al. [11], respectively:

$$n(E) = \sqrt{A\left(\frac{E_{ph}}{E_g}\right)^{-2}\left\{2-\sqrt{1+\frac{E_{ph}}{E_g}}-\sqrt{1-\frac{E_{ph}}{E_g}}\right\}+B} \quad (1)$$

$$\alpha(cm^{-1}) = 10^5\sqrt{C\cdot\left(E_{ph}-E_g\right)+D\cdot\left(E_{ph}-E_g\right)^2} \quad (2)$$

Where E_g is the bandgap, E_{ph} the incident photon energy and parameters for GaN: A=9.31, B=3.03, C=3.52517 and D=-0.65710. For GaAs, complex refractive index offering by Silvaco Atlas library was used [12].

Beside this, a set of physical models was implemented to obtain a realistic prediction of electrical behavior on simulated devices, including bandgap narrowing effect, Shockley-Read-Hall recombination model (SRH), Auger recombination model, Fermi-Dirac statistics and modified Caughey-Thomas model for mobility, similar to others reports [13-16]. Photovoltaics characteristics were measured under AM1.5 spectrum with 1 sun concentration.

After simulation of cells, characteristic parameters [17] were extracted for every device. From I-V curves, short circuit current (Isc) and open circuit voltage (Voc) were obtained; then, power curves were calculated to obtain the maximum delivered power (P_{mp}) and fill factor (FF), where:

$$FF = \frac{P_{mp}}{V_{oc}\cdot I_{sc}} \quad (3)$$

Finally, the ratio between generated electric energy and the incident light power (P_{in}) was calculated to determine the energy conversion efficiency of the cell (η) by:

$$\eta = \frac{\mathrm{Voc}\cdot I_{sc}\cdot FF}{P_{in}} \quad (4)$$

(a)

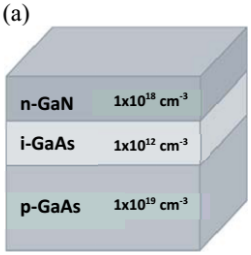

Layer	Thickness (nm)				
n-GaN	200		300		500
i-GaAs	0	50	100	200	400
	600	800	1000	1200	1500
	2000	2500	3000	5000	8000
p-GaAs	500	1000	2000	10*	350*

*Thickness in μm

(b)

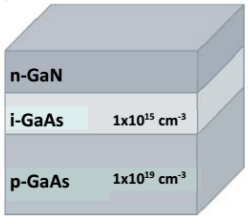

Layer	Doping (cm^{-3})		
n-GaN	$1x10^{18}$	$1x10^{19}$	$1x10^{20}$

Layer	Thickness (nm)				
i-GaAs	0	50	200	600	1000
	1200	1500	2500	5000	8000
p-GaAs	200		2000		350*

*Thickness in μm

Figure 1: GaN/GaAs heterostructures simulated. (a) Thicknesses variation of the three layers, (b) variation on doping of n-GaN layer and thicknesses of i-GaAs and p-GaAs layers.

Table 1: Physical parameters for GaAs and c-GaN used for the device simulation (T=300 K).

PARAMETER	GaAs [17]	c-GaN [18]
E_g	1.42 eV	3.2 eV
τ_n	1 ns	1 ns
τ_p	20 ns	1 ns
Nv	$7x10^{18}$ cm^{-3}	4.15×10^{19} cm^{-3}
Nc	$4.7x10^{17}$ cm^{-3}	1.195×10^{18} cm^{-3}
χ	4.07 eV	4.1 eV
ε_r	12.4	8.9
a_0	5.6532 Ă	4.52 Ă
Aug_n	$5x10^{-30}$ $cm^6 \cdot s^{-1}$	$1.5x10^{-30}$ $cm^6 \cdot s^{-1}$
Aug_p	$1x10^{-31}$ $cm^6 \cdot s^{-1}$	$1.5x10^{-30}$ $cm^6 \cdot s^{-1}$
$\mu_{n\ (min-max)}$	-	5-295 $cm^2V^{-1}cm^{-1}$
$\mu_{p\ (min-max)}$	-	170-1460 $cm^2V^{-1}cm^{-1}$

3. RESULTS

In order to analyze the behavior of energy bands in *n-GaN/i-GaAs* and *i-GaAs/p-GaAs* interfaces, Figure 2 shows the energy band diagram of three heterostructures with different thickness on *i-GaAs* layer. For *n-GaN/i-GaAs* interface, no discontinuities were observed between the valence band (Ec) and conduction band (Ev) in the three heterostructures; this can be attributed to the proximity of electron affinity for GaN and GaAs, as this prevents the bending of the bands at the interface of the heterojunction and allows a good fit between them, which contributes to good electrical conduction within the heterostructure; this feature observed in the *GaN/GaAs* heterojunctions can be considered an advantage over some other GaN-based heterostructures previously reported where there have been marked discontinuities in their energy bands [14-16].

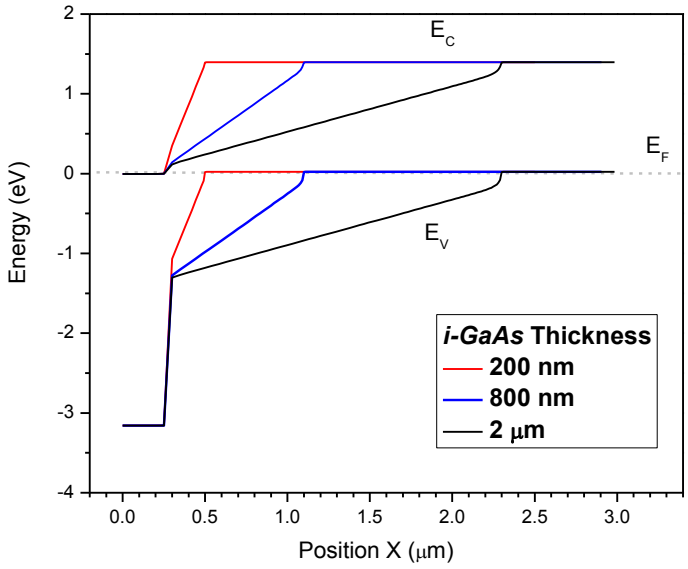

Figure 2: Energy band diagram for samples with *i-GaAs* layer thickness of 200 nm (red line), 800 nm (blue line) and 2000 nm (black line); with *n-GaN*=300 nm and *p-GaAs*=2 μm.

Current-voltage (I-V) curves were obtained and grouped by *p-GaAs* layer thickness; Figure 3 shows I-V curves for different heterostructures with thickness of 200 nm (3a) and 350 μm (3b) for *p-GaAs* layer, while *n-GaN* layer is fixed at 300 nm and *i-GaAs* is varied at different thickness. For I-V curves with *p-GaAs*=200 nm, maximum voltage was 0.98 V for *n-p* type heterostructure; however, with the increase of *i-GaAs* layer thickness, this was decreasing to 0.76 V for the heterostructure with the thicker *i-GaAs* layer of the group. By contrast, for current density a marked increase was observed with increasing the thickness of *i-GaAs* layer between 0 and 600 nm, which was subsequently decreasing to reach a maximum current density that remained of ~ 32 mA/cm^2 for the last four heterostructures (2500 to 8000 nm). In the I-V curves with *p-*

GaAs=350 µm, higher values for voltage and current density in *n-p* type heterostructure were observed. The maximum value of voltage was ~ 1.06 V corresponding to *n-p* type heterostructure; while for the current density, the maximum values were located in ~32.5 mA/cm^2 by heterostructures with the thicker *i-GaAs* layer.

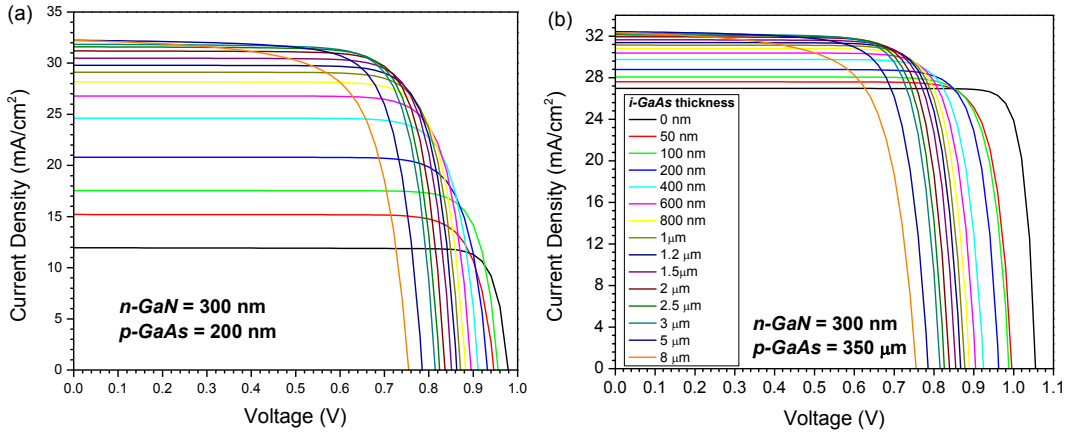

Figure 3: I-V curves for n-i-p heterostructures with different thicknesses of i-GaAs and p-GaAs=200 nm (a) and 350 µm (b); fixing n-GaN=300 nm.

Furthermore from I-V curves, the short circuit current (I_{sc}) and open circuit voltage (V_{oc}) was extracted for all heterostructures; I_{sc} as a function of *i-GaAs* layer thickness is shown in Figure 4 for different heterostructures in stage I of theoretical analysis. For different thicknesses of the *p-GaAs* layer it was initially observed a marked increase by extending the thickness of *i-GaAs* layer, to a maximum value, which lasted until the 8000 nm. Additionally, slightly higher I_{sc} values were observed with increasing thickness of the *p-GaAs*; however, for the thicknesses of 10 and 350 µm this shift disappeared. Increased I_{sc} for different thicknesses of *p-GaAs* was more remarkable for the thickness of *i-GaAs* between 0 and 1000 nm, as from 1200 nm, the I_{sc} peaked and the shift due to the thickness of the *p-GaAs* layer was diminished. Moreover, a similar behavior of I_{sc} for different thicknesses of the *n-GaN* layer (300 nm, 200 nm and 500 nm), where a maximum I_{sc} at ~32 mA/cm^2 around 3000 nm for all three thicknesses was observed. In addition, the influence of doping in *n-GaN* layer was analyzed for heterostructures simulated in stage II (Figure 5), where a maximum I_{sc} of ~ 32 mA/cm^2 was observed, but this time around 2500 nm of *i-GaAs* layer thickness. These results establish that the thickness and doping of *n-GaN* layer not greatly influence the behavior of I_{sc} in these heterostructures.

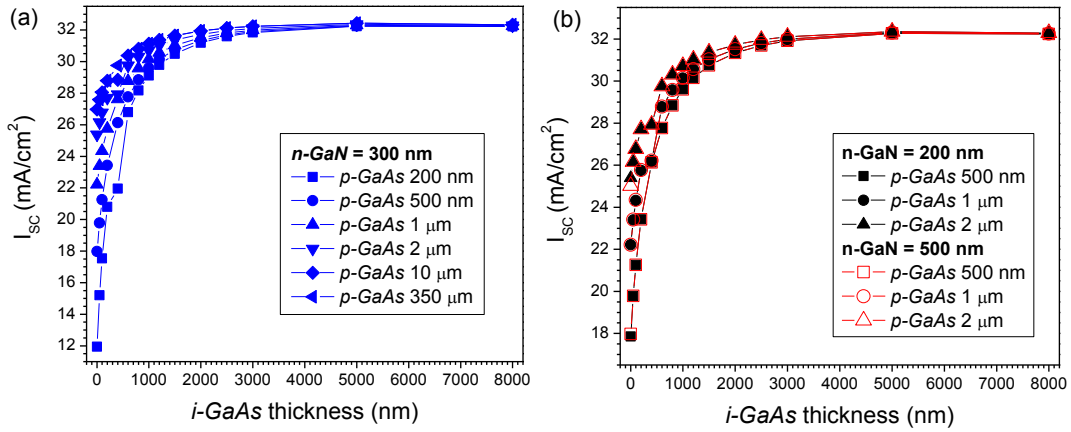

Figure 4: Variation of short circuit current (Isc) by increasing *i-GaAs* layer thickness for different *p-GaAs* thicknesses; fixing (a) *n-GaN*=300 nm, (b) 200 nm and 500 nm.

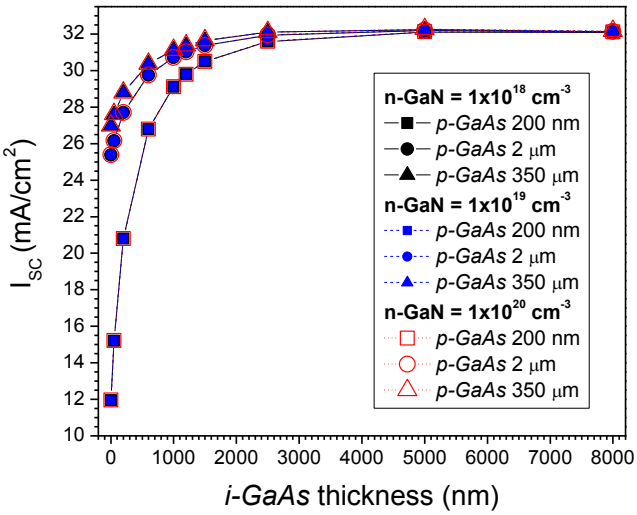

Figure 5: Variation in short circuit current (Isc) by increasing the thickness of *i-GaAs* layer using different thicknesses of *p-GaAs*; fixing *n-GaN* layer thickness to 300 nm and doping of $1x10^{18}$ cm^{-3}, $1x10^{19}$ cm^{-3} and $1x10^{20}$ cm^{-3}.

Regarding to V_{oc} (Figure 6), by increasing the thickness of *i-GaAs* layer a decrease was observed for different thicknesses of *p-GaAs*; however, although a variation in V_{oc} was found in smaller *i-GaAs* thicknesses, this remained the same in the case of thicker than 600 nm, even for different thicknesses of the *p-GaAs* layer. The highest values of V_{oc} were observed at ~ 1.06 V, corresponding to the n-p type heterostructures, even for different thicknesses of the *n-GaN* layer. In the case of heterostructures simulated during stage II with different doping in the *n-GaN* layer (Figure 7), no significant changes were observed. Higher values for V_{oc} were again corresponding to the n-p type heterostructures with thicknesses of 2 and 350 μm; which they reached values of ~ 1.05 and 1.06 V, respectively. Just as with the I_{sc}, these results confirm that both, the thickness and doping of the *n-GaN* layer, not significantly influence the V_{oc} for this kind of heterostructures.

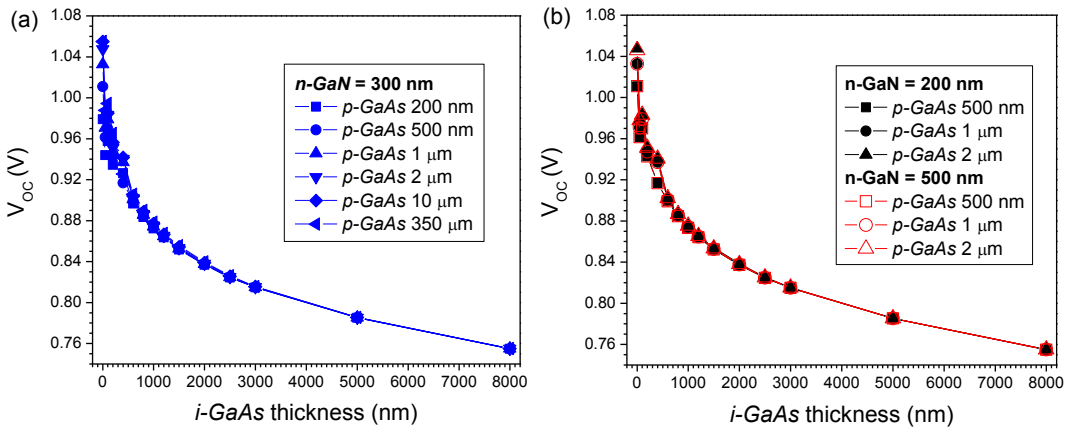

Figure 6: Open circuit voltage (V_{oc}) behavior while the thickness of *i-GaAs* layer increases for different thickness of *p-GaAs*; with *n-GaN* layer set at (a) 300 nm, (b) 200 nm and 500 nm.

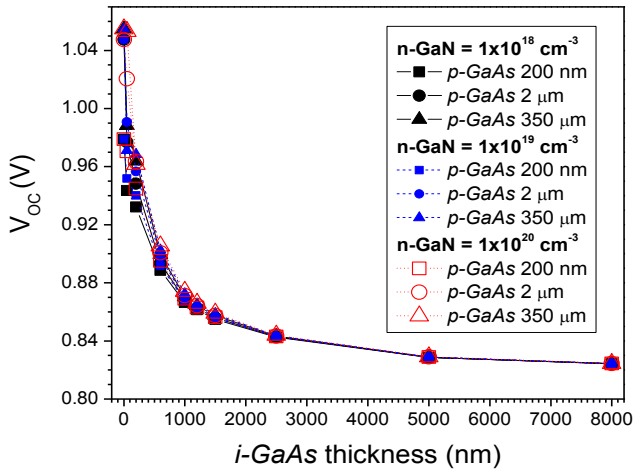

Figure 7: Open circuit voltage behavior by increasing *i-GaAs* layer thickness for different *p-GaAs* thicknesses and *n-GaN* layer thickness fixed to 300 nm with doping of $1x10^{18}$ cm^{-3}, $1x10^{19}$ cm^{-3} and $1x10^{20}$ cm^{-3}.

For fill factor parameter (FF), Figure 8 shows the results obtained in stage I simulations. Similarly to the V_{oc}, in the FF, by increasing the thickness of *i-GaAs* layer a decrease of this value was observed; however, in this case it showed an abrupt decrease between the *n-p* type heterostructure and *n-i-p* type heterostructure with a thickness of 50 nm on *i-GaAs* layer and subsequently increased for the thickness of 100 nm. The maximum FF found was ~ 0.89, for n-p type heterostructures; however, for the n-i-p type heterostructures with an *i-GaAs* thickness less than 2000 nm, values were above 0.80, a value considered acceptable for the proper performance of a solar cell [19]. In the case of i-GaAs thicknesses between 400 and 1500 nm, variation in FF was minimal; however, for thicknesses greater than 2000 nm, this decreased considerably, reaching values below 0.70 for heterostructures with *i-GaAs* thicknesses of 8000 nm. This may be caused by the increase in recombination of carriers due to excessive thickness of the *i-GaAs* layer [20], which consequently reduces the V_{oc} and the "perpendicularity" of I-V curve. For heterostructures with different layer thicknesses in *n-GaN*, no differences were observed on FF; reaffirming once again that the thickness of this layer does not impact significantly on the parameters of the cells studied.

In heterostructures where doping of *n-GaN* layer was varied (Figure 9), similarly no significant changes occurred between them; however, for the case of heterostructures with $1x10^{19}$ cm^{-3} doping in *n-GaN* layer, the FF decrease in those with thicknesses of 50 nm was much greater with respect to the other. The minimum FF was obtained in heterostructures with 600 nm of thickness on *i-GaAs* layer for doping of $1x10^{18}$ and $1x10^{20}$ cm^{-3}, while for *i-GaAs* thicknesses greater than 2000 nm this remained around 0.83. These results confirm the impact of V_{oc} in the performance of the heterostructure and the importance in maintaining a symmetrical relationship between I_{sc} and V_{oc}. Finally, for heterostructures with $1x10^{19}$ cm^{-3} doping, the minimum FF was found for the heterostructure with 50 nm of thickness on *i-GaAs* layer and further a FF of ~ 0.84 was observed for the heterostructure with an *i-GaAs* layer thickness of 200 nm and *p-GaAs* of 350 μm, indicating that the relationship between V_{oc} and I_{sc} is more proportional than in other heterostructures and therefore its "perpendicularity" is greater.

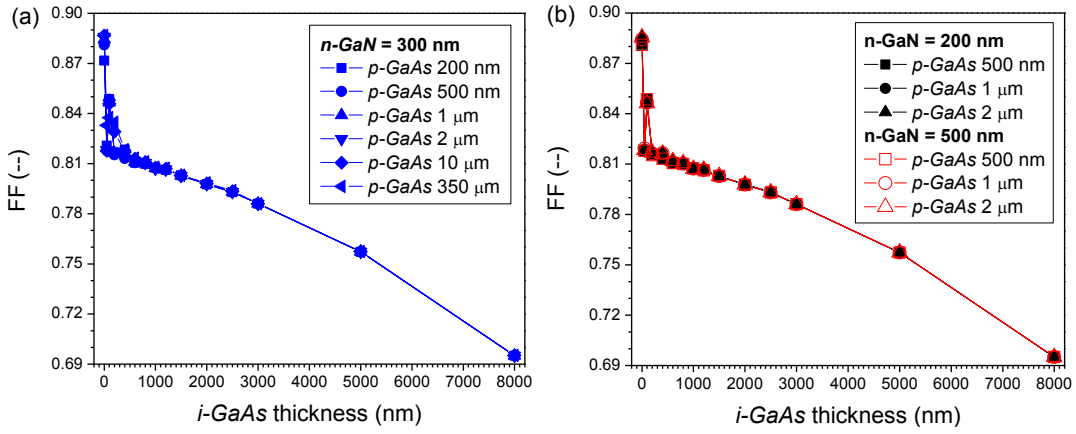

Figure 8: Variation of fill factor (FF) relative to the increased *i-GaAs* layer thickness for different *p-GaAs* thicknesses;

fixing (a) n-GaN=300 nm, (b) 200 nm and 500 nm.

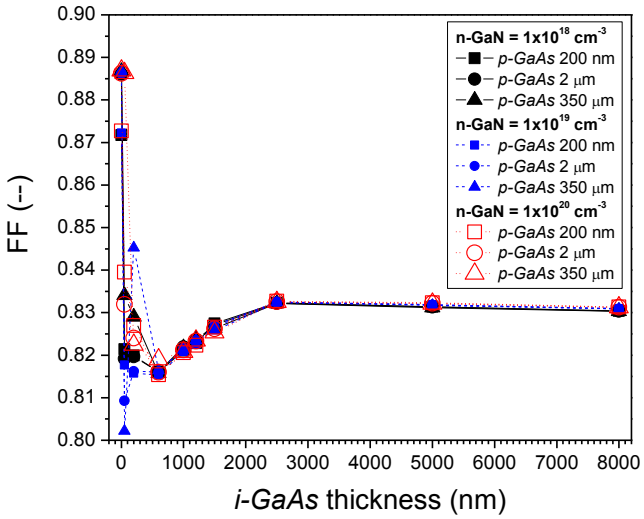

Figure 9: Variation of fill factor (FF) relative to the increase in *i-GaAs* layer thickness for different *p-GaAs* thicknesses and fixing *n-GaN* layer thickness to 300 nm and doping at $1x10^{18}$ cm^{-3}, $1x10^{19}$ cm^{-3} and $1x10^{20}$ cm^{-3}.

Theoretical efficiency of simulated cells was calculated, the efficiencies obtained in stage I are shown in Figure 10. For a *p-GaAs* layer thickness lower than 2 μm, an increase in efficiency was observed by increasing the thickness of *i-GaAs* layer to reach a peak and then a marked decrease was showed; in contrast, for *p-GaAs* thicknesses of 10 and 350 μm, the maximum efficiency values were obtained for *n-p* type heterostructures and as the thickness of *i-GaAs* layer increased the efficiency decreased. It was also found that for *i-GaAs* thicknesses greater than 2500 nm, the efficiencies reach similar values regardless the thickness of *p-GaAs* layer; reaching down to 18% for *i-GaAs* thicknesses of 8000 nm. As with the parameters discussed above, no significant changes were observed in efficiencies for heterostructures with different thicknesses in the *n-GaN* layer. Generally, the maximum values of efficiency for simulated heterostructures during stage I, reached values of ~ 25% for *n-p* and between 21 and 23% for *n-i-p* types heterostructures. In the case of heterostructures simulated during stage II (Figure 11), a similar pattern was observed, greater efficiencies were found by increasing *p-GaAs* layer thickness, reaching maximum of ~ 25.5% for *n-p* type heterostructures; however, no significant variations between different doping of *n-GaN* layers were observed. This corroborates what had already been observed in the parameters previously reported that both, the change in doping and thickness, do not generate significant changes in the performance of devices based on this type of heterostructures.

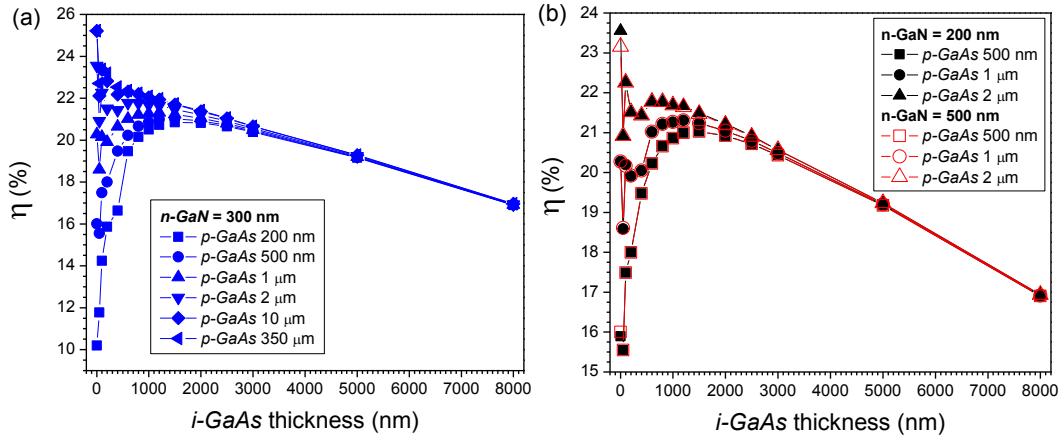

Figure 10: Variation of energy conversion efficiency (η) by increasing *i-GaAs* layer for different *p-GaAs* thicknesses with *n-GaN* fixed at (a) 300 nm, (b) 200 nm and 500 nm.

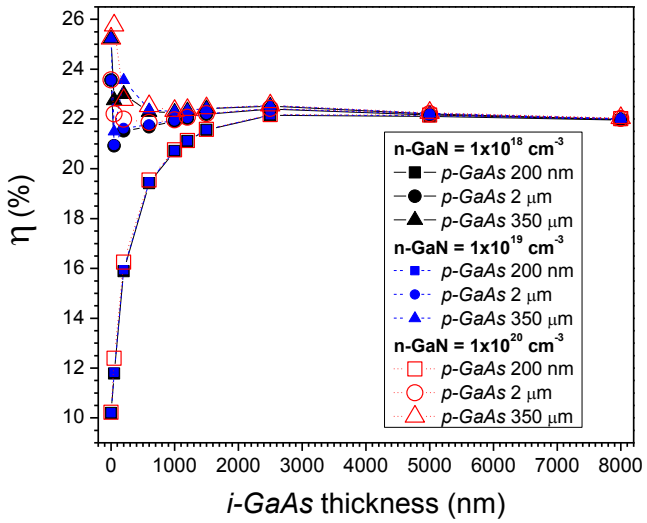

Figure 11: Variation in energy conversion efficiency (η) by increasing the *i-GaAs* layer for different *p-GaAs* thicknesses; setting the *n-GaN* doping at $1x10^{18}$ cm^{-3}, $1x10^{19}$ cm^{-3} and $1x10^{20}$ cm^{-3}; with 300 nm in thickness.

4. DISCUSSION

Although the different results presented in I-V curves, it was possible to observe similar behavior within each group; in both, as the thickness of the intrinsic layer was increased, the voltage was decreased and current density increased, which coincides with some previously works reported for photovoltaic devices based on GaN [14]. However, although the increase in current density peaked around 32 mA/cm^2 for both groups, a marked difference was observed in the increase of current density for heterostructures with *i-GaAs* layer thicknesses lower than 400 nm for the reduced thickness of *p-GaAs*. This allows argue that the thickness of the *i-GaAs* layer has a greater influence on the performance of the heterostructure when the thickness of the substrate (*p-GaAs*) is lower; however, when much greater thicknesses are used for the *p-GaAs* layer, the intrinsic layer rather affects the performance of the cell as the voltage is decreased considerably and no significant increase is generated in current density.

By knowing that I_{sc} is related to the collection of carriers, photogeneration and diffusion of carriers in the device [21], it is possible to assume that the observed increase by increasing the thickness of the *i-GaAs*, is due to an increase in absorption and therefore improved collection device and photogeneration; which it is even more pronounced for thinner *p-GaAs* thickness. Also, since Voc corresponds to maximum available voltage in the cell produced for a current density I=0, and depends on the saturation current of the cell and the photogenerated current [22], the decrease observed in the V_{oc}, can be attributed to the decrease of the electric field, due to the increased thickness of *i-GaAs* layer when n-GaN and p-GaAs layer thicknesses are fixed, which impacts the collection of carriers in the contacts of the cell and the increase in the saturation current due to recombination within the device.

According to previously reported works in n-i-p and p-i-n solar cells, the increase in the thickness of the intrinsic layer increases absorption and efficiency [16]; because when the thickness of the *i-GaAs* increases, this occupies increasingly greater extent the space charge region, and finally the region is located entirely within the intrinsic layer, which achieves a better quantum efficiency internal to the device. The results obtained in this theoretical study show that to locate the space charge within the intrinsic region, it is required a thickness between 1 and 1.5 microns for *i-GaAs*, which allows to assume that the intrinsic layer thickness must be at most the order of the absorption length, about 1.2 microns according to what was reported by Nawaz & Ahmad [14]; also, it was observed that increasing excessively the thickness of *i-GaAs* layer negatively impacts V_{oc}, because the intensity of the internal electric field is reduced and there is an increase in possibilities of recombination of carriers. Therefore, this allows justify why for thicknesses greater than the intrinsic layer, the efficiency peaks that could be attributed to absorption maximum and photogeneration, which subsequently decreases when after that peak only increases recombination and it impacts negatively in device performance.

Since this study is the first presenting an approach to the behavior of a GaN/GaAs heterostructure as photovoltaic device, it is not possible to compare the obtained results with some solar cell of this type previ-

ously reported; however we can make a comparison with cells based on GaAs and GaN previously reported separately. For GaN based solar cells, these have recently reported theoretical efficiencies between 18% and 24% [14-16] for *p-i-n* type configuration; and between 18% [11] and 26% [23] in *p-n* type cells; while cells based on GaAs have reported efficiencies between 17% and ~ 24% [24]. These values serve as a guideline for considering acceptable the results obtained in this study and allow demonstrating the potential of a GaN/GaAs heterostructure by introducing efficiencies above those previously reported for cells based on GaN and GaAs separately in multijunction devices with the advantage that this study shows this efficiencies for a single heterojunction solar cell.

5. CONCLUSIONS

In this work, we analyzed electrical behavior for a new proposed GaN/GaAs heterostructure based on cubic GaN (c-GaN) as a photovoltaic cell by numerical finite element simulations. We study the photovoltaic response for different heterostructures by obtaining their I-V curves and characteristic parameters, first by varying thickness on the three layers and then fixing the *n-GaN* layer thickness and varying the doping concentration. Simulated results showed that thickness of *i-GaAs* layer have the greater influence in device performance for thinner substrates (*p-GaAs*), and for thicker *p-GaAs* layer, the increment on intrinsic layer thickness could affect the performance by the increment of recombination inside the heterostructures. We also found that in the case of *n-GaN* layer, thickness and doping concentration do not generate significant changes in the performance of devices based on this type of heterostructures. However, results shows efficiencies between 23 and 25% for *n-i-p* and *n-p* heterostructures and the potential of designing improved heterostructures for c-GaN/GaAs solar cells using GaAs as a substrate.

6. ACKNOWLEDGMENTS

The authors want to thank DGDAIE-UV, DGI-UV, and SENER-CONACYT for their support of this work.

7. BIBLIOGRAPHY

[1] KANG, M.S., LEE, C.H., PARK, J.B., *et al.*, "Gallium nitride nanostructures for light-emitting diode applications", *Nano Energy*, v. 1, n. 3, pp. 391–400, 2012.

[2] HARIMA, H., "Properties of GaN and related compounds studied by means of Raman scattering", *Journal of Physics Condensed Matter*, v. 14, n. 38, pp. R967–R993, 2002.

[3] BHUIYAN, A.G., SUGITA, K., HASHIMOTO, A., YAMAMOTO, A. "InGaN solar cells: Present state of the art and important challenges", *IEEE Journal of Photovoltaics*, v. 2, n. 3, pp. 276–293, Jul. 2012.

[4] PERLIN, P., SUSKI, T., TEISSEYRE, H., *et al.,* "Towards the identification of the dominant donor in GaN", *Physical Review Letters*, v.75, n. 2, pp. 296–299, Jul. 1995.

[5] LIU, L., EDGAR, J.H. "Substrates for gallium nitride epitaxy", *Materials Science and Engineering R*, v. 37, n. 3, pp. 61–127, 2002.

[6] WU, M.H., CHANG, S.P., CHANG, S.J., *et al.*, "Characteristics of GaN/InGaN double-heterostructure photovoltaic cells", *International Journal of Photoenergy*. v. 2012, pp. 206174/1-5, 2012.

[7] ZAINAL, N., NOVIKOV, S. V., AKIMOV, A. V., *et al.*, "Hexagonal (wurtzite) GaN inclusions as a defect in cubic (zinc-blende) GaN", *Physica B: Condensed Matter*, v. 407, n. 15, pp. 2964–2966, 2012.

[8] LIU, H.F., CHEN, H., LI, Z.Q., *et al.,* "MBE growth and Raman studies of cubic and hexagonal GaN films on (001)-oriented GaAs substrates", *Journal of Crystal Growth*, v. 218, pp. 191–196, 2000.

[9] MÖREKE, J., UREN, M.J., NOVIKOV, S.V., *et al.* "Investigation of the GaN-on-GaAs interface for vertical power device applications", *Journal of Applied Physics*, v. 116, pp. 014502/1-6 , 2014.

[10] PIPREK, J., *Nitride semiconductor devices. Principles and simulation,* 1 ed., Weinheim, WILEY-VCH Verlag GmbH & Co. KGaA, 2007.

[11] BROWN, G.F., AGER, J.W., WALUKIEWICZ, W., WU, J., "Finite element simulations of compositionally graded InGaN solar cells", *Solar Energy Materials and Solar Cells,* v. 94, n. 3, pp. 478–483, 2010.

[12] SILVACO INC., *Atlas User's Manual,* Santa Clara, CA, 2014.

[13] DEL ÁNGEL-LARA, A., ALONSO-RODRÍGUEZ, M., HERNÁNDEZ-QUIROZ, T., *et al.,* "Effects of Capping and Intrinsic Layers on Current Density in PIN and NIP GaN/InGaN/GaN Solar Cells", *Energy and Environment Focus*, v. 2, n. 4, pp. 315–319, 2013.

[14] NAWAZ, M., AHMAD, A., "A TCAD-based modeling of GaN/InGaN/Si solar cells", *Semiconductor Science and Technology*, v. 27, pp. 035019/1-9, 2012.

[15] MAHALA, P., RAY, A., JANI, O., DHANAVANTRI, C., "Theoretical study on the effect of graded $In_yGa_{1-y}N$ layer on p-GaN/$In_yGa_{1-y}N$/n-GaN p-i-n solar cell". *Physica Status Solidi A*, v. 210, n. 12, pp. 2656–2661, 2013.

[16] NACER, S., AISSAT, A., "Simulation of InGaN p-i-n double heterojunction solar cells with linearly graded layers", *Optik*, v. 126, n. 23, pp. 3594–3597, 2015.

[17] SZE, S.M., NG, K.K., *Physics of Semiconductor Devices*, 3 ed., Hoboken, NJ, John Wiley & Sons, Inc., 2007.

[18] PEARTON, S.J., ABERNATHY, C.R., REN, F., *Gallium Nitride Processinf for Electronics, Sensors and Spintronics*, 1 ed., Gainesville, FL, Springer, 2008.

[19] GREULICH, J., GLATTHAAR, M., REIN, S., "Fill factor analysis of solar cells' current-voltage curves", *Progress in Photovoltaics: Research and Applications*, v. 18, n. 7, pp. 511–515, 2010.

[20] HAMEDANI, P.F., TAGHINIA, A., YAZDI, F., ARTIMANI, Z.M., "Study the effect of varying the thickness of intermediate band on the intermediate band solar cells efficiency" In: *Energy Procedia of 2nd International Conference on Advances in Energy Engineering (ICAEE)*, pp. 1496–1502, Bangkok, Thailand, 2012.

[21] NELSON, J., *The Physics of Solar Cells*. 1 ed., London, UK, Imperial College Press, 2003.

[22] WÜRFEL, P., *Physics of solar cells: from basic principles to advanced concepts*, 1 ed., Weinheim, WILEY-VCH Verlag GmbH & Co. KGaA, 2005.

[23] MESRANE, A., RAHMOUNE, F., MAHRANE, A., OULEBSIR, A., "Design and Simulation of InGaN p-n Junction Solar Cell", *International Journal of Photoenergy*, v. 2015, pp. 594858/1-9, 2015.

[24] DAS, N.C., "Enhanced solar energy harvesting using top n-contact GaAs solar cell", *Solid-State Electronics,* v. 107, pp. 11–14, 2015.